Transient thermal characterization of AlGaN/GaN HEMTs under pulsed biasing

Georges Pavlidis, Dustin Kendig, Eric R. Heller, and Samuel Graham

***Abstract*— The development of steady state thermal characterization techniques for AlGaN/GaN HEMTs have been used to measure the device's peak temperature under DC conditions. Devices are, however, normally operated under pulsed bias or RF operation and thus require transient thermometry techniques to capture the device's dynamic thermal behavior. One technique that has shown the ability to achieve this is Transient thermoreflectance imaging (TTI). The accuracy of TTI is based on a using the correct thermoreflectance coefficient. In the past, alternative techniques have been used to adjust the thermoreflectance coefficient to match the correct temperature rise in the device. This work provides a new method to accurately determine the thermoreflectance coefficient of a given surface and is validated via an electrical method: gate resistance thermometry (GRT). Close agreement is shown between the temperature rise of the passivated gate metal measured by TTI and the averaged gate temperature monitored by GRT. Overall, TTI can now be used to to thermally map GaN HEMTs under pulsed conditions providing simultaneously a sub microsecond temporal resolution and a submicron spatial resolution.**

***Index Terms*— AlGaN/GaN HEMTs, self-heating, transient, Thermal Characterization, Temperature, Gate Resistance Thermometry, Thermoreflectance, Thermal Resistance**

I. INTRODUCTION

GALLIUM nitride (GaN) has shown to have great potential in high electron mobility transistors (HEMTs) for radio frequency (RF) devices [1] and high-voltage power electronics [2]. Its inherent high breakdown field strength [3] enables operating voltages and power densities much higher than that of prior technologies such as GaAs. This implies extreme localized joule heating near the gate [4] which can cause a mixture of both temporary thermally induced device performance droop and permanent degradation [5]. With previous technology such as Si and GaAs, thermal time constants were tens microseconds or longer [6]. In contrast, the thermal time constants associated with GaN have been measured to be on the order of microseconds [7]. Additionally, GaN is typically grown on a Si or SiC substrate with very different thermal diffusivity, unlike Si and GaAs for discrete power FETs. To obtain the full potential out of these devices, understanding and controlling the device transient thermal dynamics is important to their lifetime and reliability. Several thermometry techniques have been developed to estimate the peak channel temperature in GaN HEMT's [8, 9]. While spatially accurate measurement methods such as Raman have been developed to estimate the junction temperature under DC biasing conditions [10], the use of transient techniques to monitor the formation of the hotspot under pulsed/RF operation biasing have not been fully investigated [11]. Transient Raman thermography has shown to be accurate but requires multiple acquisitions to thermally map a device as it is a single point measurement [12]. Additionally, Raman is sensitive to mechanical stress; the mechanical stress environment for transiently powered GaN is complex [13]. To extract the correct time constants of GaN HEMTs, a measurement technique that possesses both high temporal and temperature resolution is necessary.

One technique that has the ability to measure simultaneously the transient surface temperature rise of both the channel and the gate metal is transient thermoreflectance [14]. The accuracy of this technique is based on how well the thermoreflectance coefficient, C_{th}, of the surface of interest can be estimated [15]. This is based on the change in reflectivity of a surface, ($\Delta R/R$), for a given temperature rise, ΔT.

$$C_{th} = \Delta T \times \left(\frac{\Delta R}{R} \right)^{-1} \quad (1)$$

Due to thermal expansion effects, heating a material without maintaining constant plane of focus to determine the C_{th} can introduce error in the measurement of reflectivity [16]. Previous studies have used a combination of electro-thermal modelling and Raman thermometry to adjust the C_{th} of the metal to match the expected results [16-18]. While this methodology for validating transient thermoreflectance is accurate, the procedure requires additional complex equipment and long acquisition times. Recent advancements in transient thermoreflectance imaging (TTI) technology has enabled the use of a piezoelectric stage to account for thermal expansion during the extraction the C_{th} [19]. In this work, TTI is used to estimate the C_{th} of different regions on the device and

Submitted paper for review. This work was supported by the Air Force Research Laboratory led High Reliability Electronics Virtual Center (HiREV).

G. Pavlidis and S. Graham are with The George W. Woodruff School of Mechanical Engineering, Georgia Institute of Technology, Atlanta, GA 30332 USA (email: sgraham@gatech.edu)

D. Kendig is with Microsanj LLC, Santa Clara, CA, 95051 USA

E.R. Heller is with the Materials and Manufacturing Directorate, Air Force Research Laboratory, Wright Patterson Air Force Base, OH 45433 USA..

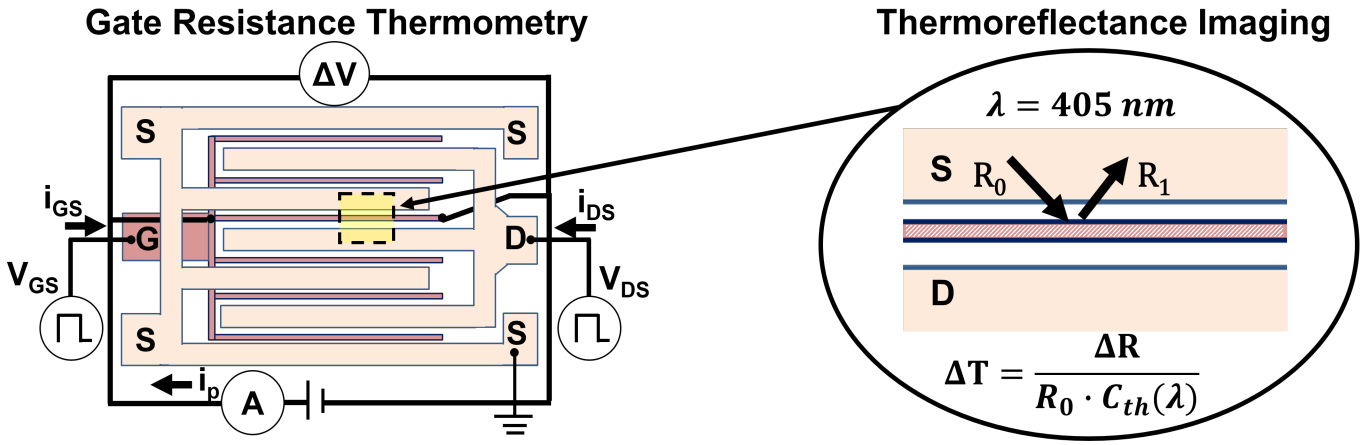

Fig. 1. Four terminal sensing gate resistance thermometry device in pulsed bias configuration. For direct comparison to transient thermoreflectance imaging, simultaneous thermoreflectance mapping of the device gate width was performed. A 405 nm LED excitation source was pulsed to measure the transient thermoreflectance response.

investigate the device's transient thermal response under pulsed bias conditions. The temperature profiles are validated via gate resistance thermometry (GRT) [20], a technique which has shown to have the potential to also monitor the transient thermal behavior of the gate metal under pulsed conditions [21, 22].

II. Experimental Details

In this study, transient thermoreflectance imaging (TTI) is used to perform surface temperature mappings of AlGaN/GaN HEMTs on a SiC substrate. The devices tested were six fingered devices with a 370 µm gate width and were identical to the devices measured via gate resistance thermometry in [20]. A Microsanj NT220B was used to perform the measurements [19]. Since the C_{th}, is both material and excitation source wavelength dependent [15], the addition of passivation layers on top of the GaN channel and the gate metal can alter the C_{th} leading to significant errors in the estimated temperature rise via TTI. The C_{th} must thus be measured for every surface studied instead of attempting to estimate the coefficient theoretically with approximations of the different layer thicknesses and material composition. Furthermore, estimating the true temperature of the surface when measuring the reflectivity can also lead to error in the coefficient. To overcome this issue, a thermocouple was placed directly on the die of the device instead of using the thermocouple in the Peltier stage. A wavelength sweep was performed to determine the optimal wavelength that results in the highest thermoreflectance signal for the regions around the GaN channel. Performing the calibration at approximately a 100 °C temperature rise, all regions resulted in a strong C_{th} for a 405 nm LED source (C_{th} = -2.4 x 10^{-4} $°C^{-1}$ for the gate metal, C_{th} = -3 x 10^{-4} $°C^{-1}$ for the source and drain contact and C_{th} = -2.1 x 10^{-4} $°C^{-1}$ for the GaN region). Due to the small gate footprint, the calibration measurements were taken at 50x and 100x magnification.

Similar to the setup described in [20], the devices were biased under pulsed conditions using an AMCAD Pulsed IV system as shown in Figure 1. A 20 V 400-µs period pulse was applied to the drain with varying duty cycle from 10-40%. A constant pulsed gate bias was applied to prevent errors in the gate resistance measurements due to change in the leakage currents. A 10 µs delay was applied to ensure that the gate bias was applied before the drain bias (Figure 2b). The maximum power dissipated was estimated to be 3.9 W/mm. For TTI, an LED pulse width of 5.5 µs (Figure 2) was used to obtain a strong consistent thermoreflectance signal on the regions of interest. Temperature rises were recorded every 8 µs from 10 to 270 µs. To account for any accumulated heating in the package during pulsed biasing, a thermocouple was placed near the package to monitor any temperature rise. The temperature rise estimated via TTI was thus always referenced to the true base temperature. Using an 100x magnification lens, the autofocusing function used for calibrations could also be applied to the TTI imaging reducing the uncertainty in the CCD imaging. While this limits the region of interest to approximately a quarter of the device gate width (Figure 1), a clear thermoreflectance signal can be obtained from the gate.

To verify the accuracy of this technique, a 4-point transient electrical characterization method using the gate metal resistance was performed simultaneously to TTI. The voltage drop across the gate finger was measured using a Tektronix DPO3012 Oscilloscope and a probe current of 3 mA was applied. Gate resistance thermometry (GRT) measurements were performed every 2 minutes capturing 4 periods each time. An average of all the waveforms captured was taken to directly compare to the TTI temperatures estimated above the gate region. The standard error of the GRT uncertainty was calculated using 95% confidence intervals.

III. Experimental Results and Discussion

To directly compare the temperature measured by TTI to GRT, thermoreflectance images using a 100x lens were taken of the central measured GRT finger. An example of the temperature rise monitored across the gate via TTI is shown in Figure 2. The images shown were accumulated over 80 seconds at LED time delays of 15.2 µs and 167.2 µs respectively. Noting the applied 10 µs delay to the drain bias, Figure 2b captures the temperature rise at the very beginning of the pulse, between 2.5 µs and 8 µs after the drain bias is applied. The image shows that the highest temperature is

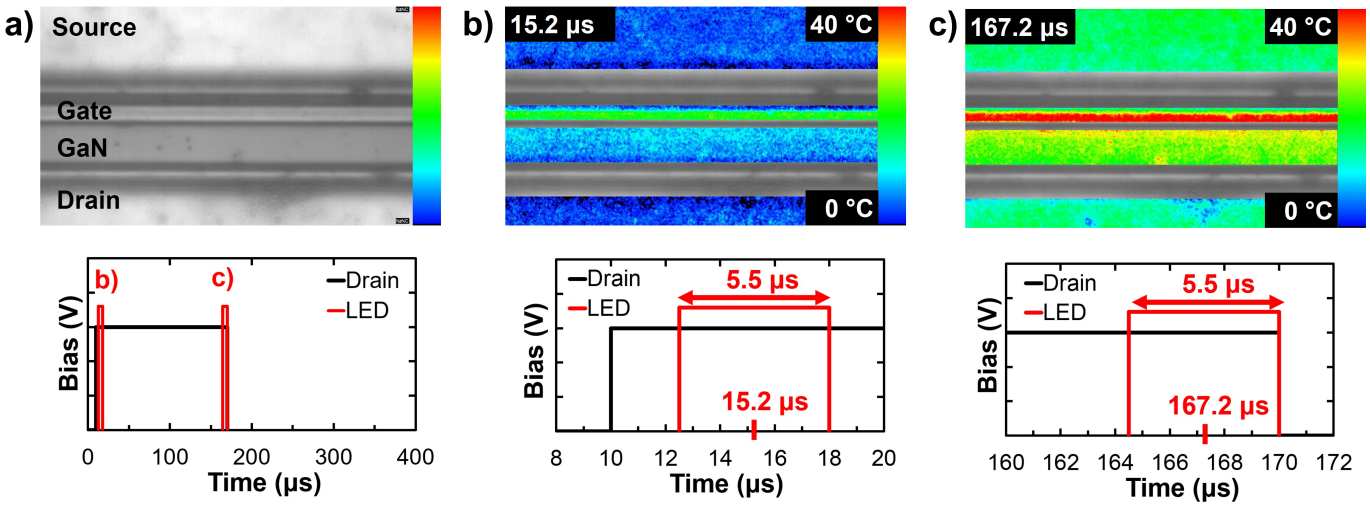

Fig. 2. a) CCD image of 6x370 µm GaN HEMT including timing synchronization between device bias and LED pulse. LED pulse widths of 5.5 µs were applied at time delays of b) 15.2 µs and c) 167.2 µs. The corresponding CCD based thermoreflectance image highlights the area of localized joule heating along the gate width during pulsing.

found to be along the gate width confirming the localized joule heating profile present in GaN HEMTs. Figure 2c represents closely the peak temperature rise in the device at the end of the pulse when a 40% duty cycle is applied. The peak surface temperature in the device remains over the gate metal region as expected. The heat is shown to spread along the channel where a temperature gradient can be seen along the GaN channel. The drain and source pads appear to have the lowest temperature rise as they are furthest away from the source of localized joule heating. Temperature data from pixels located over the edges of the ohmic and Schottky contacts were filtered due to low intensity of light reflected from these areas which translated into large uncertainties.

Acquiring images every 8 µs, the gate temperature rise and decay of the device under 10%, 20% and 40% duty cycle was monitored. To directly compare the temperature rise using TTI with transient GRT, an averaged probed region across the gate width was used and plotted in Figure 3.

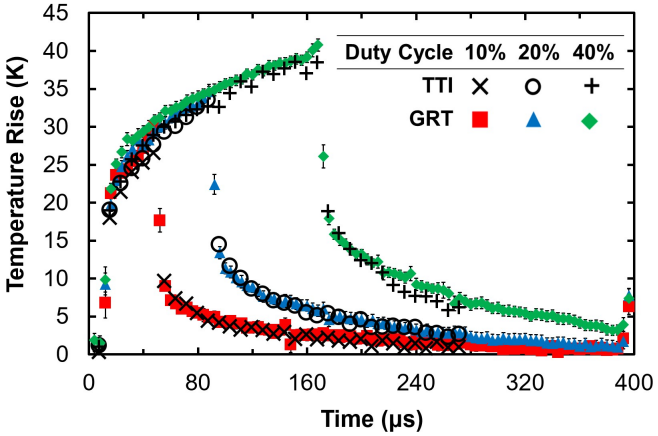

Fig. 3. Comparison of transient thermal response of GaN HEMT under various duty cycles measured by Transient Thermoreflectance Imaging, TTI (markers) and Gate Resistance Thermometry, GRT (shapes).

The averaged region would represent approximately the same temperature the GRT method is measuring when averaging over the gate metal resistance. The close agreement between the TTI and GRT measurements (maximum 5% difference) indicates that the gate metal C_{th} extracted from the calibration is accurate.

The overall base temperature rises when increasing the duty cycle. This is shown in Figure 4 where the absolute base and peak temperature of the device is plotted against the average power dissipated. The base temperature in the device represents the gate temperature when no power is dissipated (drain bias is off) and is shown to rise by 26 °C when increasing the duty cycle from 10% to 40%. The increase in base temperature captured by GRT highlights one of the advantages of using this method over thermoreflectance to capture the absolute device temperature. Furthermore, comparing the 26 °C temperature rise to the package temperature rise of 2 °C measured by the thermocouple indicates that the heating caused under pulsed biasing conditions is primarily dissipated in the die.

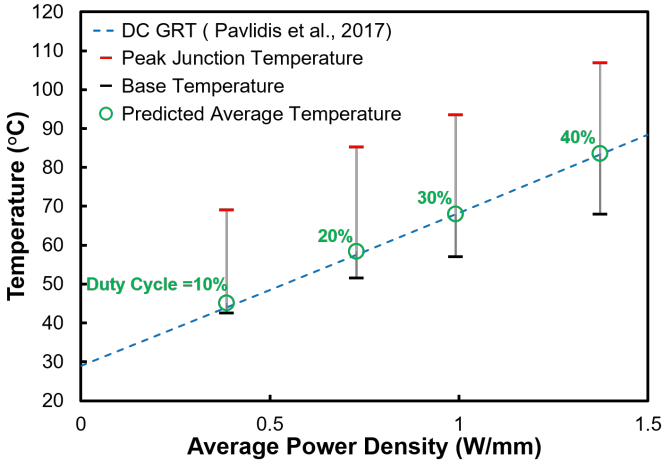

Fig. 4. Absolute base and peak temperature measured by GRT for varying duty cycle from 10% to 40% with a time period of 400 us. A calculated average gate temperature is compared to DC GRT results measured for the same device.

Using linear interpolation, the average temperature of the gate metal over a pulse can be calculated using the duty cycle applied and the base and peak temperature measured. The results of these averaged temperatures are directly compared

in Figure 4 to the GRT measurements previously conducted under DC biasing [20]. The close agreement between these two values for all duty cycles show the potential of using DC GRT, a simpler technique, to estimate the peak temperature under pulsed biasing. Although this DC approach will limit extracting thermal time constants and understanding the device's transient thermal dynamics, it could give a rough estimate of the device's maximum temperature under pulsed biasing.

The thermoreflectance coefficients can now be used to monitor the temperature rise across the whole device including the GaN, Drain and Source regions (Gate C_{th}: -2.5 x 10^{-4} $°C^{-1}$, Drain and Source C_{th}: -3 x 10^{-4} $°C^{-1}$ and GaN C_{th}: -2.1 x 10^{-4} $°C^{-1}$). Using these values with a 20x magnification lens, a device thermal mapping is shown in Figure 5. The temperature profile along the gate width for the middle gate finger and bottom gate finger are plotted. The temperature profile along the middle gate finger shows a significant temperature rise from 23.2 °C at the edge of the mesa to 42.6 °C in the center. As shown in [20], the averaged GRT temperature (40 °C) does not capture this gradient showing the necessity of a mapping technique such as TTI to capture the peak temperature and gradient. Furthermore, the uneven temperature distribution between fingers is shown in Figure 5. In contrast to the middle gate finder, a 8.8 °C temperature gradient along the bottom gate finger is observed.

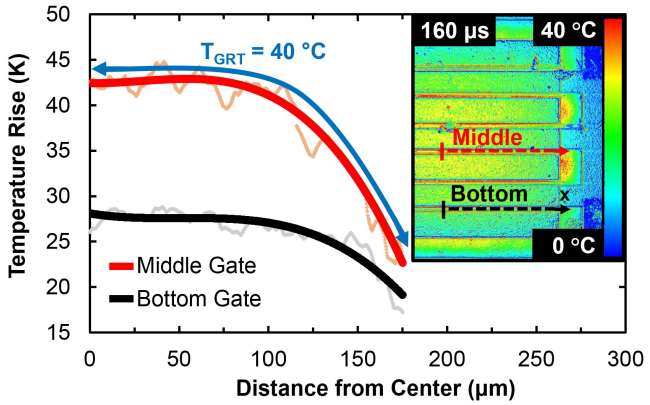

Fig. 5. Temperature profile along gate width of middle gate finger and bottom gate finger. Temperature profiles were extracted from thermal image measured by Transient Thermoreflectance Imaging using a 20x lens. The blue line represents the averaged area that was probed using transient Gate Resistance Thermometry (GRT). The device was biased for a 400 µs period with a 40% duty cycle.

IV. Conclusion

Overall, the averaged temperature across the gate width measured by TTI shows close agreement with the transient GRT results. For a constant drain and gate bias, the gate metal temperature rise and decay under pulsed biasing is monitored with varying duty cycles from 10 to 40%. The results highlight the accuracy of using an advanced autofocusing function to extract the correct thermoreflectance coefficient of the passivated gate metal. The comparison of the transient temperature swing to previous DC GRT results indicates that the peak temperature can be roughly estimated by extrapolating from the steady state DC temperature. Providing an accurate method to employ TTI enables the possibility of extracting thermal time constants to better understand the thermal properties of GaN HEMTs. In contrast to transient GRT, TTI has proven to be advantageous for temperature mappings of the device providing submicron spatial resolution. These mapping techniques will enable direct evaluation of adjusting device geometries such as gate to gate spacing and gate width to improve thermal spreading throughout the device.

Acknowledgment

This work was supported by the Air Force Research Laboratory High-Reliability Electronics Virtual Center (HiREV) team and AFOSR under award number FA9550-17RXCOR434.

References

[1] U. K. Mishra, P. Parikh, and Y.-F. Wu, "AlGaN/GaN HEMTs-an overview of device operation and applications," *Proceedings of the IEEE,* vol. 90, pp. 1022-1031, Jun 2002,doi: https://doi.org/10.1109/JPROC.2002.1021567

[2] E. A. Jones, F. Wang, and B. Ozpineci, "Application-based review of GaN HFETs," in *Wide Bandgap Power Devices and Applications (WiPDA), 2014 IEEE Workshop on*, 2014, pp. 24-29. doi: https://doi.org/10.1109/WiPDA.2014.6964617

[3] B. J. Baliga, "Power Semiconductor-Device Figure of Merit for High-Frequency Applications," *IEEE Electron Device Letters,* vol. 10, pp. 455-457, Oct 1989,doi: https://doi.org/10.1109/55.43098

[4] S. Choi, E. R. Heller, D. Dorsey, R. Vetury, and S. Graham, "The impact of bias conditions on self-heating in AlGaN/GaN HEMTs," *IEEE Transactions on Electron Devices,* vol. 60, pp. 159-162, Jan 2013,doi: https://doi.org/10.1109/Ted.2012.2224115

[5] M. G. Ancona, S. C. Binari, and D. J. Meyer, "Fully coupled thermoelectromechanical analysis of GaN high electron mobility transistor degradation," *Journal of Applied Physics,* vol. 111, p. 074504, Apr 1 2012,doi: https://doi.org/10.1063/1.3698492

[6] Y. Qiao, S. Feng, C. Xiong, X. Ma, H. Zhu, C. Guo, and G. Wei, "The thermal properties of AlGaAs/GaAs laser diode bars analyzed by the transient thermal technique," *Solid-State Electronics,* vol. 79, pp. 192-195, Jan 2013,doi: https://doi.org/10.1016/j.sse.2012.07.007

[7] K. R. Bagnall, O. I. Saadat, S. Joglekar, T. Palacios, and E. N. Wang, "Experimental Characterization of the Thermal Time Constants of GaN HEMTs Via Micro-Raman Thermometry," *IEEE Transactions on Electron Devices,* vol. 64, pp. 2121-2128, May 2017,doi: https://doi.org/10.1109/Ted.2017.2679978

[8] S. A. Merryman and R. Nelms, "Diagnostic technique for power systems utilizing infrared thermal imaging," *IEEE Transactions on Industrial Electronics,* vol. 42, pp. 615-628, Dec 1995,doi: https://doi.org/10.1109/41.475502

[9] R. J. Simms, J. W. Pomeroy, M. J. Uren, T. Martin, and M. Kuball, "Channel temperature determination in high-power AlGaN/GaN HFETs using electrical methods and Raman spectroscopy," *IEEE Transactions on Electron Devices,* vol. 55, pp. 478-482, Feb 2008,doi: https://doi.org/10.1109/Ted.2007.913005

[10] S. Choi, E. R. Heller, D. Dorsey, R. Vetury, and S. Graham, "Thermometry of AlGaN/GaN HEMTs using multispectral raman features," *IEEE Transactions on Electron Devices,* vol. 60, pp. 1898-1904, Jun 2013,doi: https://doi.org/10.1109/Ted.2013.2255102

[11] J. W. Pomeroy, M. J. Uren, B. Lambert, and M. Kuball, "Operating channel temperature in GaN HEMTs: DC versus RF accelerated life testing," *Microelectronics Reliability,* vol. 55, pp. 2505-2510, Dec 2015,doi: https://doi.org/10.1016/j.microrel.2015.09.025

[12] M. Kuball and J. W. Pomeroy, "A Review of Raman Thermography for Electronic and Opto-Electronic Device Measurement With Submicron Spatial and Nanosecond Temporal Resolution," *IEEE Transactions on Device and Materials Reliability,* vol. 16, pp. 667-684, Dec 2016,doi: https://doi.org/10.1109/Tdmr.2016.2617458

[13] J. P. Jones, E. Heller, D. Dorsey, and S. Graham, "Transient stress characterization of AlGaN/GaN HEMTs due to electrical and thermal effects," *Microelectronics Reliability,* vol. 55, pp. 2634-2639, Dec 2015,doi: https://doi.org/10.1016/j.microrel.2015.08.019

[14] K. Maize, E. Heller, D. Dorsey, and A. Shakouri, "Fast transient thermoreflectance CCD imaging of pulsed self heating in AlGaN/GaN power transistors," in *Reliability Physics Symposium (IRPS), 2013 IEEE International*, 2013, pp. CD. 2.1-CD. 2.3. doi: https://doi.org/10.1109/IRPS.2013.6532059

[15] T. Favaloro, J.-H. Bahk, and A. Shakouri, "Characterization of the temperature dependence of the thermoreflectance coefficient for conductive thin films," *Review of Scientific Instruments,* vol. 86, p. 024903, Feb 2015,doi: https://doi.org/10.1063/1.4907354

[16] S. Martin-Horcajo, J. W. Pomeroy, B. Lambert, H. Jung, H. Blanck, and M. Kuball, "Transient Thermoreflectance for Gate Temperature Assessment in Pulse Operated GaN-Based HEMTs," *IEEE Electron Device Letters,* vol. 37, pp. 1197-1200, Sep 2016,doi: https://doi.org/10.1109/Led.2016.2595400

[17] L. Baczkowski, J. C. Jacquet, O. Jardel, C. Gaquiere, M. Moreau, D. Carisetti, L. Brunel, F. Vouzelaud, and Y. Mancuso, "Thermal Characterization Using Optical Methods of AlGaN/GaN HEMTs on SiC Substrate in RF Operating Conditions," *IEEE Transactions on Electron Devices,* vol. 62, pp. 3992-3998, Dec 2015,doi: https://doi.org/10.1109/Ted.2015.2493204

[18] K. Maize, G. Pavlidis, E. Heller, L. Yates, D. Kendig, S. Graham, and A. Shakouri, "High resolution thermal characterization and simulation of power AlGaN/GaN HEMTs using micro-Raman thermography and 800 picosecond transient thermoreflectance imaging," in *Compound Semiconductor Integrated Circuit Symposium (CSICs), 2014 IEEE*, 2014, pp. 1-8. doi: https://doi.org/10.1109/CSICS.2014.6978561

[19] D. Kendig, A. Tay, and A. Shakouri, "Thermal analysis of advanced microelectronic devices using thermoreflectance thermography," in *Thermal Investigations of ICs and Systems (THERMINIC), 2016 22nd International Workshop on*, 2016, pp. 115-120. doi: https://doi.org/10.1109/THERMINIC.2016.7749037

[20] G. Pavlidis, S. Pavlidis, E. R. Heller, E. A. Moore, R. Vetury, and S. Graham, "Characterization of AlGaN/GaN HEMTs Using Gate Resistance Thermometry," *IEEE Transactions on Electron Devices,* vol. 64, pp. 78-83, Jan 2017,doi: https://doi.org/10.1109/Ted.2016.2625264

[21] J. Kuzmík, S. Bychikhin, M. Neuburger, A. Dadgar, A. Krost, E. Kohn, and D. Pogany, "Transient thermal characterization of AlGaN/GaN HEMTs grown on silicon," *IEEE Transactions on Electron Devices,* vol. 52, pp. 1698-1705, Aug 2005,doi: https://doi.org/10.1109/Ted.2005.852172

[22] B. K. Schwitter, A. E. Parker, S. J. Mahon, and M. C. Heimlich, "Transient gate resistance thermometry demonstrated on GaAs and GaN FET," in *Microwave Symposium (IMS), 2016 IEEE MTT-S International*, 2016, pp. 1-4. doi: https://doi.org/10.1109/MWSYM.2016.7540035

Georges Pavlidis received his M.Eng degree in Mechanical Engineering from Imperial College London, United Kingdom. He is currently working towards the Ph.D deegree in the Woodruff School of Mechanical Engineering at the Georgia Institute of Technology.

His current research interests include assessing the reliability of GaN transistors using optical and electrical techniques.

Dustin Kendig is currently Vice President of Engineering at Microsanj, where he is developing submicron transient thermal imaging systems. He received his B.S. with honors in Electrical Engineering from the University of California, Santa Cruz where his research focused on using thermoreflectance imaging to characterize microscopic defects in photovoltaics, heating in power transistor arrays, and thermoelectric devices.

Eric Heller received the Ph.D. degree in physics from The Ohio State University, Columbus, OH, USA, in 2003.

His current research interests include physics based modeling of electrical, thermal, and stress effects in wide bandgap devices.

Samuel Graham received the Ph.D. degree in mechanical engineering from the Georgia Institute of Technology, Atlanta, GA, USA, in 1999.

He is currently a Professor and Rae S. and Frank H. Neely Professor within the Woodruff School of Mechanical Engineering, Georgia Institute of Technology and holds a joint appointment with the Energy and Transportation Science Division of Oak Ridge National Laboratory.